Article

Porous Polysulfone/Activated Carbon Capsules as Scaffolds for Enzyme Immobilization

Magdalena Olkiewicz [1,*], Josep M. Montornes [1], Ricard Garcia-Valls [1,2], Iwona Gulaczyk [3] and Bartosz Tylkowski [1,*]

1   Eurecat, Centre Tecnològic de Catalunya, Chemical Technologies Unit, Marcel·lí Domingo 2, 43007 Tarragona, Spain; josep.montornes@eurecat.org (J.M.M.); ricard.garcia@urv.cat (R.G.-V.)
2   Department of Chemical Engineering, Universitat Rovira i Virgili, Av. Països Catalans 26, Campus Sescelades, 43007 Tarragona, Spain
3   Faculty of Chemistry, Adam Mickiewicz University in Poznań, ul. Uniwersytetu Poznańskiego 8, 61-614 Poznań, Poland; iwona.gulaczyk@amu.edu.pl
*   Correspondence: magda.olkiewicz@eurecat.org (M.O.); bartosz.tylkowski@eurecat.org (B.T.)

Abstract: Enzymes play a vital role in various industrial sectors and are essential components of many products. Hybrid enzyme-polymeric capsules were developed using polysulfone-activated carbon capsules as scaffolds. The polysulfone-activated carbon capsules with an average diameter of 2.55 mm were fabricated by applying a phase inversion precipitation method. An increase in the amount of immobilized enzymes was observed with growth of activated carbon amount in polysulfone matrix. Enzyme immobilization was confirmed by the Bradford method, while Viscozyme® L activity in carboxymethyl cellulose hydrolysis to glucose was measured by the Reducing Sugar DNS method. The recycling of the hybrid Viscozyme® L-polysulfone/activated carbon capsules, and their reuse for subsequent cellulose hydrolysis was investigated and demonstrated repeatability of results.

Keywords: enzyme immobilization; polysulfone-activated carbon capsules; phase inversion precipitation; polisulfone; Viscozyme® L

1. Introduction

Enzymes are crucial in various industrial sectors and are key components of many products. In 2019, the global enzyme market was valued at USD 9.087 billion. It is projected to grow to USD 13.815 billion by 2027, with a compound annual growth rate (CAGR) of 6.4% from 2020 to 2027 [1]. The term "enzyme" was proposed by Wilhelm Kuhne in 1877 [2], which in Greek means "leavened" or "in yeast"; however, enzymology began in the 19th century with the gradual understanding of the mechanisms of digestion and fermentation [3]. The use of natural enzymes for food processing and preservation dates back to ancient times, including bread-making in Egypt and fermentation practices across Eastern cultures [4]. Over time, enzyme applications transitioned from traditional practices to systematic scientific research, revealing their chemical properties and establishing the theoretical basis of enzyme engineering. Enzyme engineering flourished in the late 20th century with advances in molecular biology and genetic engineering. However, large-scale production faces challenges as harsh solvent systems and mechanical stress often reduce enzymes' thermal stability and catalytic activity, limiting industrial applications. Furthermore, as researchers deepen their understanding of enzyme structure and function, they increasingly recognize the importance of optimizing enzyme performance to enhance

catalytic efficiency and meet specific industrial demands. Consequently, various optimization techniques have emerged, including genetic engineering, chemical modification (such as covalent modification, cross-linking, and immobilization), directed evolution, natural enzyme screening and modification, and artificial enzyme development [1,5,6].

Immobilized enzymes offer greater resistance to environmental changes and can be easily recovered and recycled compared to their free counterparts. The main advantage of immobilization is that it protects enzymes from harsh conditions, such as high temperatures and extreme pH levels. Furthermore, enzyme immobilization reduces the dissolution of enzyme subunits, preventing deactivation and enhancing process performance and stability [7]. Moreover, immobilization facilitates their reuse, allows their easy separation from the product, and increases adaptability to changing conditions [8]. Historically, the immobilization of enzymes has been essential to the commercial viability of many large-scale biocatalytic processes [9,10]. Besides immobilized enzymes have been used in other numerous large-scale industries. Examples include glucose isomerase for the production of high fructose corn syrup, penicillin G amidase for the production of semisynthetic antibiotics, the use of lipases for the production of cocoa butter analogs, and the production of chiral amines in organic solvents, all at scales ranging from multi-thousand to multi-hundred thousand tons per annum. The glucose isomerase process involves the conversion of 10^7 tons of glucose per annum. However, it is worth noting that glucose production involves the conversion of 10^9 tons of corn starch per annum using soluble amylases [11,12]. Other examples include; detergent, paper, and textile sectors [13,14]. In addition, in biotechnology, the search for biocompatible and efficient enzyme immobilization methods has gained significant attention, especially for applications in biosensors development [15] and biodiesel production [16].

There are many different methods used for enzyme immobilization; however, the industry perpetually chooses simple and cost-effective methods. Thus, the most used approaches are based on physical immobilization (adsorption or physical entrapment) and chemical immobilization [17]. Enzyme immobilization can be achieved using a variety of matrices. These matrices are categorized based on their origin into three types: organic supports (both natural and synthetic), inorganic supports (both natural and synthetic), and hybrid supports (comprising materials of both organic and inorganic origin) [18].

On the one hand, among these various supports, natural organic matrices have been widely utilized because of their low synthesis and application costs. Activated carbon/biochar has been identified as a great support due to its high surface area, good chemical, and thermal stability, hydrophilicity, and insolubility, which are important characteristics for application in an industrial scale. Antanasković et al. [19] investigated the laccase immobilization on biochar gained from sour cherry stones and evaluates its application for brilliant green degradation. The authors reported that biochar can effectively be used as an enzyme carrier and be further utilized for the removal of emerging pollutants, positioning it as a sustainable solution for wastewater treatment. De Almeida et al. [20] studied the process of immobilization of lipase from Burkholderia cepacia by physical adsorption on graphene oxide derived (GO) from grape seed biochar. The authors demonstrated a high potential of graphene oxide obtained from biochar in immobilization lipase, especially in the application of nanobiocatalysts on an industrial scale.

On the other hand, in recent decades, different enzyme–polymer immobilization methodologies have arisen, including adsorption or entrapment on/into solid polymeric particles, metal–organic frameworks, fibers, hydrogels, and polymeric capsules [21–23]. It has been demonstrated that embedding enzymes into macroscopic polymeric structures offers several benefits. Generally, the larger the enzyme-polymeric hybrid, the greater its

recycling potential, which significantly enhances the overall economy of the biocatalytic process [24].

The aim of this work was to develop porous polymeric/activated carbon capsules as scaffolds for enzyme immobilization. Polysulfone was selected as the polymeric matrix to fabricate the capsule due to its thermal stability, strong mechanical strength, and good chemical resistance [25,26]. Polysulfone is a semihydrophobic material, containing sequential aromatic and aliphatic units that repulse water and hydrophilic compounds. The occasional hydrophilic character of its product surface is provided by the oxygen (aryl-O-alkyl) and sulfur dioxide (aryl-SO$_2$-alkyl) moieties that are able to form hydrogen bonds. This polymer was launched in 1965 as BAKELITE® Polysulfone [27]. In the literature its biocompatibility has also been proven [28], as well as its application in encapsulation technology development [29–31].

The capsules were prepared by a phase inversion precipitation method which is the most widely used membrane preparation method [32,33]. Phase inversion is a demixing process in which an initially homogeneous polymer solution is transformed from a liquid state to a solid state in a controlled manner during which the membrane structure, properties, and chemical interaction depend on the choice of polymer, as does the choice of additives used in the casting solution [34]. In case of encapsulation technology, a polymeric mixture of solvent and active materials plus solvent is propped in a coagulation bath containing nonsolvent. Due to the solvent and nonsolvent exchange, precipitation takes place and the formation of capsule structures with entrapped active materials occurs [35].

2. Materials and Methods

2.1. Materials

Activated carbon Norit (Norit® CA1, chemically activated, powder prepared from wood, ref: 97876), polysulfone (average Mw ~35,000, average Mn ~16,000), carboxymethyl cellulose (medium viscosity, ref. 21902) and Viscozyme® L (Cell Wall Degrading Enzyme Complex from *Aspergillus* sp., Lysing Enzyme from *Aspergillus* sp., ref: V2010), sodium acetate (99.995% trace metals basis, ref. 229873), dinitrosalicylic acid reagent (used in colorimetric determination of reducing sugars, ref. D0550), sodium hydroxide (puriss. p.a., ACS reagent, reag. Ph. Eur., K $\leq$ 0.02%, $\geq$98%, pellets, ref. 30620), and D-(+)-glucose ($\geq$99.5%, ref. G8270) were provided by Sigma-Aldrich (Madrid, Spain). *N,N*-Dimethylformamide (DMF, extra Pure, ref: D/3840/17) was purchased from Fisher Scientific (Madrid, Spain), while Quick Start Bradford protein assay was provided by Bio-Rad (Madrid, Spain). All reagents were used as received, without any further modification and/or purification.

2.2. Capsules Preparation

Investigated capsules were prepared by a phase inversion precipitation method [36] from a polymeric mixture composed of 20% of polysulfone with or without the activated carbon in DMF as a solvent. The polymeric solution was prepared by dissolving 20% *w/w* of polysulfone and mixing it with different amounts of activated carbon (0–5 wt%) as it is described in Table 1. Then, the mixture was stirred at 500 rpm for 24 h at room temperature. Afterwards, the capsules were obtained by dosing 3 mL of the polymeric solution into a coagulation bath containing 100 mL of distilled water as a non-solvent. The dosing rate of polymeric solution was optimized at 0.4 mL/min using a syringe pump (KDS-410-CE, kdScientific, Holliston, MA, USA). The prepared capsules were filtered and left for one hour in a clean water bath under stirring, in order to extract the rest of DMF. Finally, the capsules were filtrated and in order to remove any potentially reminded solvent they were subsequently dried using a rotary evaporator.

Table 1. Composition of different polymeric solutions.

Sample	Polysulfone (wt%)	Carbon (wt%)	DMF (wt%)
C1	20	0	80
C2	20	0.5	79.5
C3	20	1	79
C4	20	2	78
C5	20	5	75

2.3. Capsules Characterization

Both the external and internal morphology of prepared capsules were analyzed by means of Environmental Scanning Electron Microscope (ESEM, FEI Quanta 600) in high vacuum mode, using a secondary electron detector and an accelerating voltage of 20 kV. To analyze the internal morphology, micrographs of the cross-section of capsules were taken. In order to obtain a cross-section without modifying the polymeric structure, the capsules were cryogenically cut. To carry out it first, the capsules were mixed with an embedding medium (OCT Compound) and frozen at −25 °C on an aluminum support inside the machine. Once frozen, they were cut into slices of thickness 20 μm and then they were deposited on a microscopic slide. All the cross-section images were analyzed with the ImageJ software (version 1.52, publicly available from the National Institutes of Health, Bethesda, MD, USA) in order to quantify the mean pore size and the macrovoid size of the capsules. External morphology of the capsules was also observed by optical microscopy (TE2000-E, NIKON, Melville, NY, USA) in order to visualize carbon particles in their surface. During this analysis, the capsules were not covered with any external layer as in case of ESEM. They were put on the sample holder and studied. The pictures were captured with a camera integrated with the microscope.

Additionally, the capsule weight and diameter were measured using an analytical balance (ED224S, Sartorius, Göttingen, Germany) and a digital caliper (D-42387, Forum, Wuppertal, Germany), respectively. The average capsule weight was determined based on 10 measurements. Weight compositions of dried capsules were calculated based on the mass balance of the materials used for their preparation.

Moreover, the overall capsule porosity, ε, defined as the volume of the pores divided by the total volume of the capsule, was calculated using a method based on density measurements. The overall capsule porosity was determined from bulk and polysulfone densities by using the following Equation (1):

$$\varepsilon = \left(1 - \frac{\rho_c}{\rho_{psf}}\right) \times 100\% \tag{1}$$

where ρ_c and ρ_{psf} (1.24 g/cm^3) correspond to capsule and polysulfone density, respectively.

For the capsules with activated carbon the equation is slightly different [37]:

$$\varepsilon = \left(1 - \frac{\rho_c}{\rho_{psf+ac}}\right) \times 100\% \tag{2}$$

where ρ_c is a capsule density and ρ_{psf+ac} is a weighted average of the material density, considering that density of activated carbon is 0.4 g/cm^3.

Furthermore, activated carbon, polysulfone, polysulfone capsule (C1), and polysulfone capsules with activated carbon (C5) were investigated by means of Fourier Transform Infrared Spectroscopy (FT-IR), using Jasco FT/IR-6700 Infrared Spectrometer at 4 cm^{-1} resolution and 32 scans. The wavelength range was from 400 to 4000 cm^{-1}.

2.4. Enzyme Immobilization on Capsule Surface

The immobilization of enzymes from the aqueous solution onto the capsule surface was performed in batch experiments using a 50 mL Erlenmeyer flask. 1 g of capsules was added to 25 milliliters of enzyme solution (1 g/L) and slightly stirred using a magnetic stirrer for 24 h at room temperature.

The immobilized amount of the enzymes was indirectly determined by analyzing the remaining amount of enzymes in the solutions by the standard Bradford method using UV–Vis spectrophotometer at 595 nm (UV-1800, Shimadzu, Duisburg, Germany). Quick Start Bradford protein assay kit with bovine γ-globulin at 2 mg/mL, 1.5 mg/mL, 1 mg/mL, 0.75 mg/mL, 0.5 mg/mL, 0.25 mg/mL and 0.125 mg/mL and were used to plot a calibration curve.

2.5. Efficiency of Sugar Hydrolysis by Immobilized Enzyme

The amount of glucose liberates during cellulose hydrolysis in the presence of im-mobilized Viscozyme® L was determined according to slightly modified Reducing Sugar DNS method developed by Miller [38]. First, acetate buffer 0.05 M (pH 5) was prepared by dissolving 2.886 g of sodium acetate and 0.889 g (0.847 mL) of acetic acid in 1 L of milliQ water (pH of this solution was around 4.5). Its pH was adjusted to the value 5 using 10 M NaOH. Next, 25 mL of 1 g/L of carboxymethyl cellulose in the acetate buffer (25 mL) was prepared and pre-heated to 50 °C. Then, 10 g of capsules with immobilized enzyme were added, and the mixture was heated at 50 °C for 24 h. After incubation, the reaction was terminated by adding 3 mL of 3,5-dinitrosalicylic acid reagent to 1 mL of the reaction mixture. Reducing sugars were estimated colorimetrically with 3,5-dinitrosalicylic acid using glucose as standard using UV–Vis spectrophotometer at 540 nm (UV-1800, Shimadzu, Duisburg, Germany).

3. Results and Discussion

Using a phase inversion precipitation method, five types of capsules, named C1–C5, were prepared. Their characteristics are provided in Table 2. Phase inversion is a controlled process that transforms a polymer from a solution state to a solid state. In our case, to form PSF-based capsules, activated carbon was first dispersed in DMF solutions containing 20 wt% of PSF. The resulting PSF-AC mixtures were then dropped into a coagulation bath containing water as a non-solvent. As shown in Table 2, C1 capsules were prepared without AC, while C2–C5 capsules included 2.4, 4.8, 9.1, and 20 wt% of AC in PSF structures, respectively. Sharma et al. [39] and Hosseini et al. [40] fabricated polyethersulfone membranes with activated carbon at concentrations ranging from 0 to 1 wt.%. In order to investigate the effect of AC on capsule morphologies we decided to extend its content up to 5 wt%. Obtained results demonstrated that the diameters of the capsules ranged from 2.5 to 2.6 ± 0.1 mm and were not affected by the increase in carbon content within the PSF matrix. However, their weights increased with rising carbon content, with approximately a 21% increase in weight observed when comparing capsules C1 and C5.

Table 2. Capsules characterization.

Sample	Carbon Content in Dried Capsule (%)	Capsule Diameter (mm)	Capsule Weight (mg)	Porosity (%)	Pore Diameter (μm)	Average Macrovoids Size (μm)
C1	0	2.5 ± 0.1	2.8 ± 0.1	73.4	4.9 ± 0.5	893.1 ± 439.8
C2	2.4	2.5 ± 0.1	2.9 ± 0.2	72.5	5.2 ± 0.7	412.4 ± 114.7
C3	4.8	2.6 ± 0.1	3.0 ± 0.1	72.4	4.7 ± 0.2	487.3 ± 137.8
C4	9.1	2.6 ± 0.1	3.2 ± 0.3	70.2	4.4 ± 0.5	415.3 ± 261.6
C5	20	2.6 ± 0.1	3.4 ± 0.2	65.7	5.1 ± 0.3	506.9 ± 253.0

Values are means ± SD, n = 10.

The influence of AC on the polymeric capsule structures was also analyzed in terms of internal and external morphologies by optical microscope and ESEM. The optical microscope was used in order to visualize the carbon particles in the polymeric capsule surface which were not possible to be observed in ESEM micrographs. As shown in Figure 1, the carbon modified capsule is darker due to the black carbon particles, which are clearly observed.
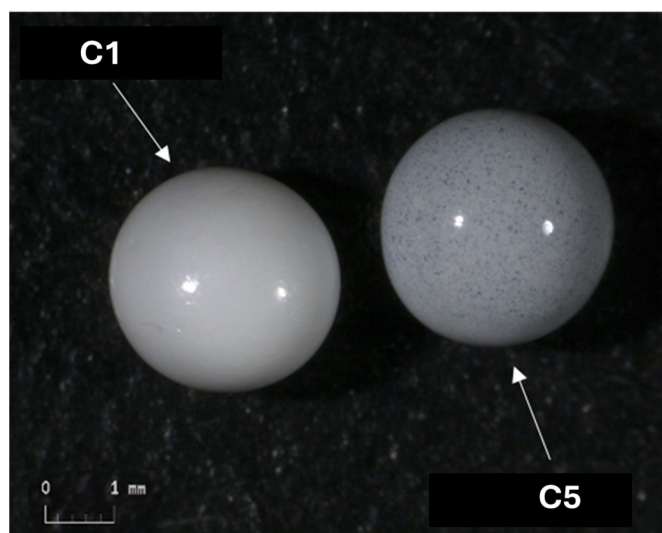

Figure 1. Optical micrographs of C1 and C5 capsules.

Figures 2 and 3 show the ESEM micrographs of surface and cross-section morphologies of C1–C5 capsules, respectively. The ESEM cross-section images demonstrate that prepared capsules are matrix type spheres. All of them possess similar porous outer morphology and spongy/finder-like internal matrix structure with macrovoids. Captured morphologies are similar to those reported by Tan and Rodrigue who used polysulfone for membrane preparation [41]. The results of capsule porosity, provided in Table 2, show a dependence on the carbon content: the higher the carbon content, the lower the porosity of the capsules. The pore sizes do not change significantly, and their value range is between 4.7 ± 0.2 and 5.2 ± 0.7 µm. However, the macrovoids are smaller in carbon capsules compared to pure polysulfone C1 capsules. As the macrovoids have different dimensions within a single capsule cross-section, the corresponding standard deviation values are very high. A similar tendency was also observed by Torras et al. [42,43] concerning the preparation of a polysulfone-activated carbon membrane with different amounts of activated carbon. Moreover, Priscila et al. [44] investigated the influence of addition of the activated carbon in the system polysulfone/NMP/water in terms of membrane morphology, hydrophilicity, thermal and mechanical resistance. The authors reported that membrane surface became denser with the addition of higher activated carbon contents.

Figure 4 provides FT-IR spectra of pure polysulfone (PFS), activated carbon, C1 and C5 capsules. The spectrum contains some important characteristics band which are visible at specific wave number. In case of pure polysulfone, C1 and C5 capsules, the C_6H_6 ring stretch is located at 1584 cm^{-1} and 1485 cm^{-1}. The asymmetric stretching vibration of C-O appears at 1235 cm^{-1}. Symmetric stretching vibration of S=O is located at 1146 cm^{-1} and 1292 cm^{-1}. The bands located at 831 cm^{-1} is due to para-disubstituted ring, i.e., C-H, out of plane bending vibration. Bands appearing in region of 721 cm^{-1} to 662 cm^{-1} results from C=C out of plane bending vibration [45]. It can be observed that spectra of polysulfone, C1 and C5 samples are the same, which confirm the original structure of pure polymer. In the case of activated carbon, the interpretation of the spectra is complicated by the fact that

each functional group generates several bands at different wavenumbers, meaning each band may contain contributions from multiple groups, as it was reported by Figueiredo et al. [46], who also noted that for carbon which is not highly oxidized, the intensity of the absorption bands in infrared spectroscopic methods is insufficient. Following the literature, the infrared bands associated with different oxygen functional groups on the activated carbon (Figure 4) were assigned. The broad band at 3600–3200 cm^{-1} can be assigned to OH from the COOH groups. This band clearly demonstrates the presence of OH groups on the surface. The bands at 1700–1500 cm^{-1} as well as 1400–900 cm^{-1} could be assigned to the following oxygen functional groups such as: carboxyl-carbonates, quinones, lactones, ethers, phenols, and carboxylic anhydrides [46,47]. The commercially available carbon used for C2–C5 capsules preparation was chemically activated by the supplier, as it is described in Section 2.1. Material. As shown in Figure 4, the presence of absorption bands in the FT-IR spectrum of carbon, associated with different oxygen functional groups, confirms its activation.
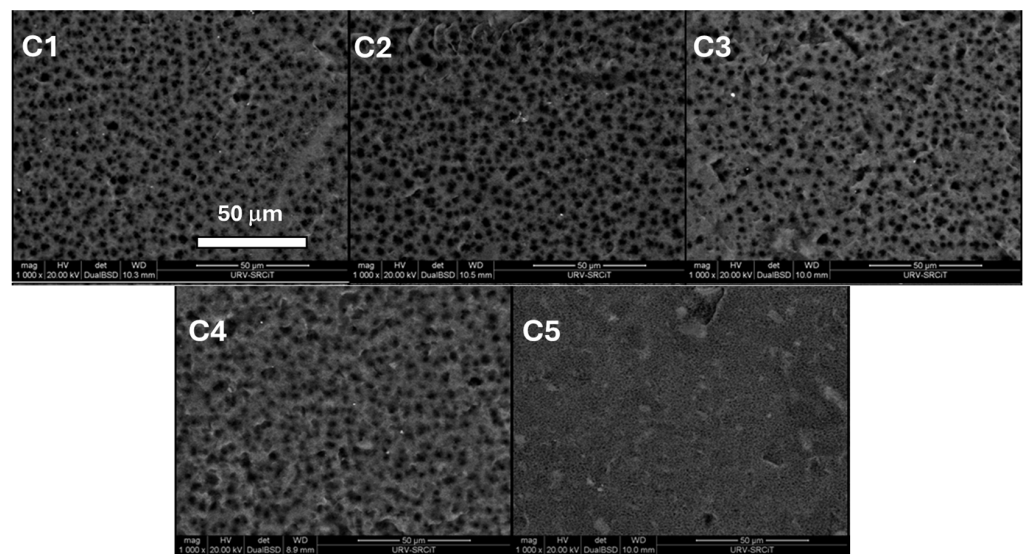

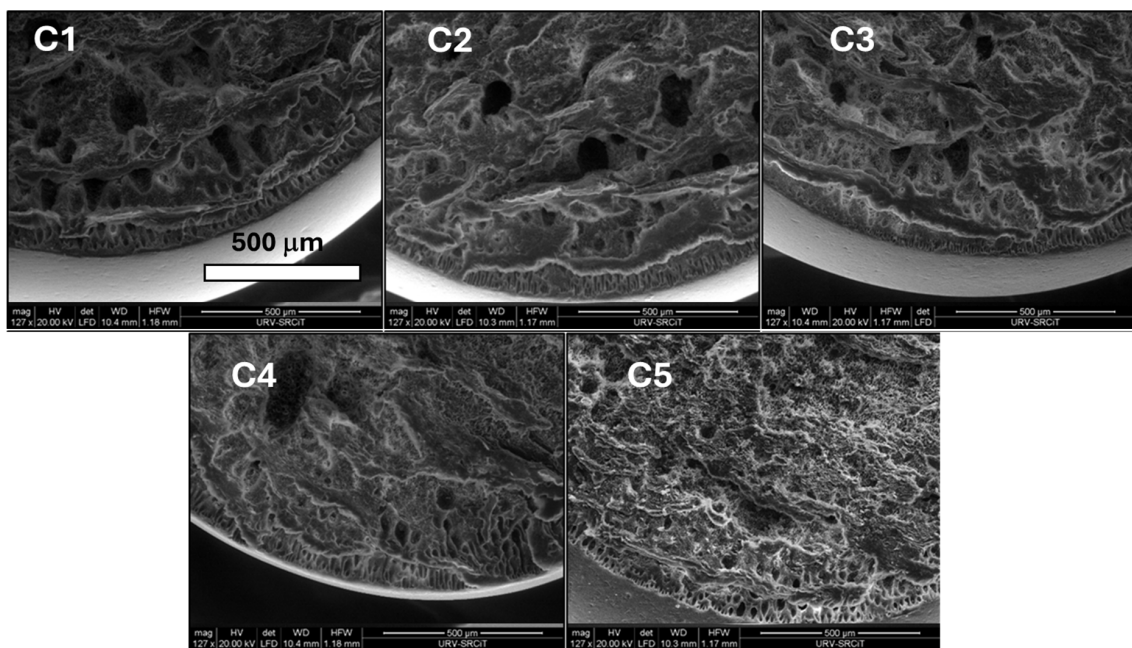**Figure 2.** ESEM micrographs of surface morphologies of C1–C5 capsules.

Figure 3. ESEM micrographs of cross-section morphologies of C1–C5 capsules.
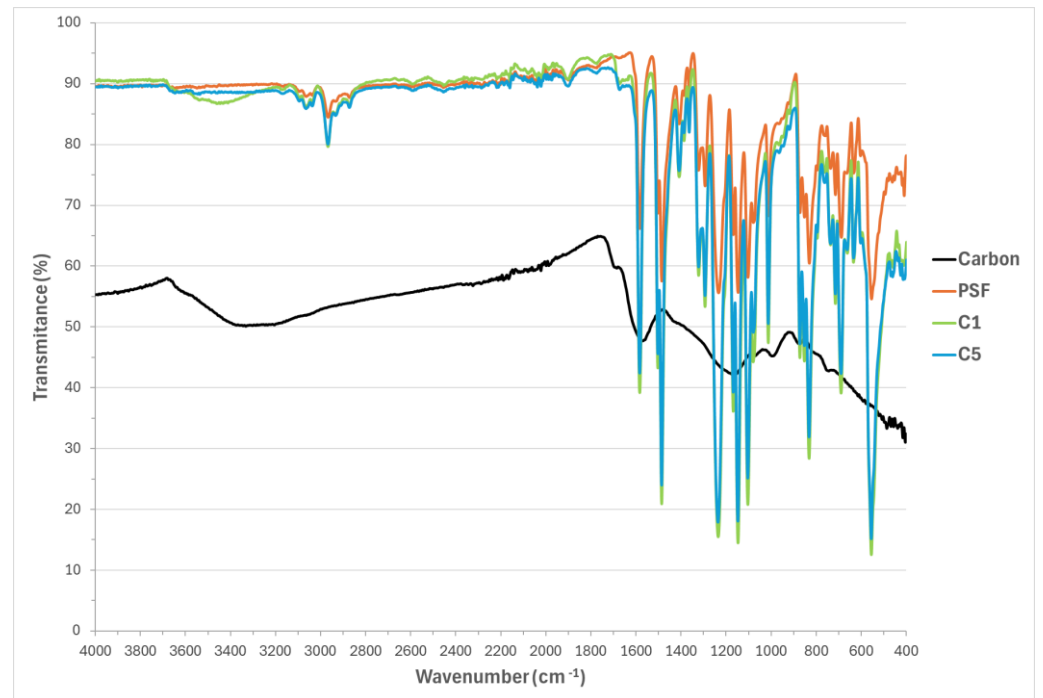
Figure 4. FT-IR spectra of pure polysulfone (PSF), activated carbon (Carbon), and capsules C1 (0% carbon) and C5 (20% carbon).

During the next step of our investigation, prepared C1–C5 capsules were used as support platforms for enzyme immobilization. In our studies, Viscozyme® L, which is a multi-enzyme complex containing a wide range of carbohydrases, including arabanase, cellulase, β-glucanase, hemicellulase, and xylanase enzymes, was immobilized on C1–C5 capsules by a physical adsorption (physisorption) process which is characterized by weak interactions between the enzyme and the capsule scaffolds. As it is given in Table 3 and Figure 5, with the higher carbon content in capsule structures, the higher amount of immobilized enzymes was achieved.
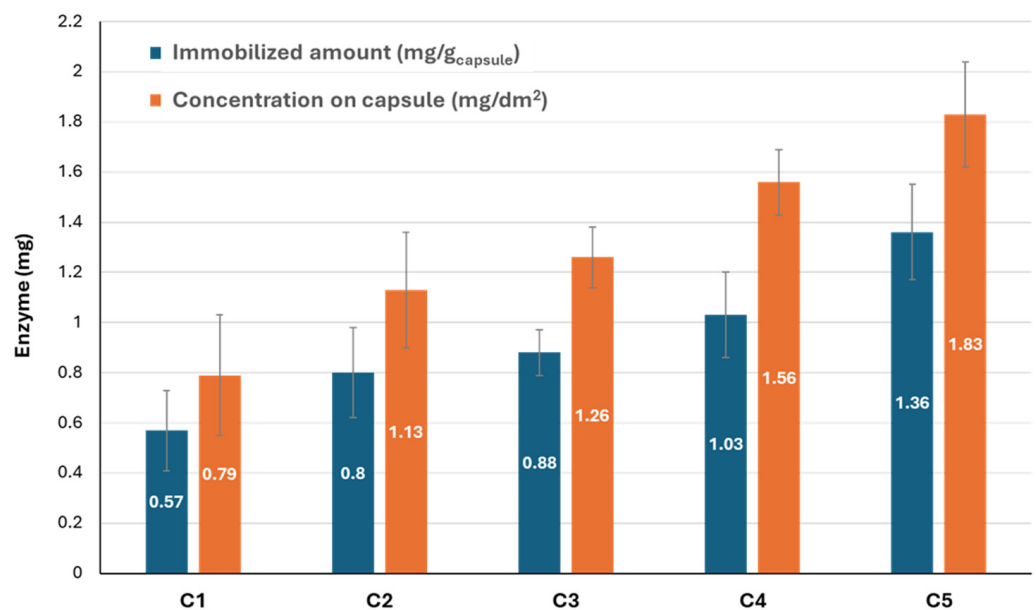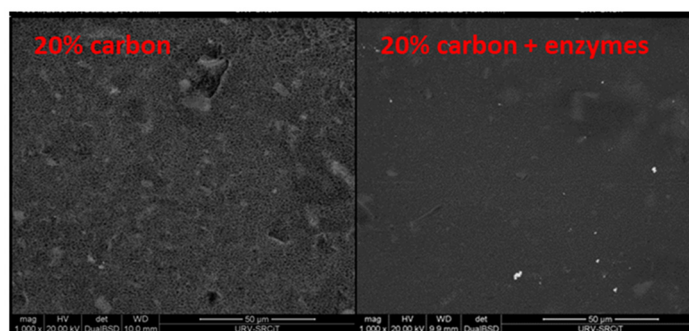

Figure 5. Enzyme Immobilization results.

Table 3. Enzyme Immobilization results.

Sample	Carbon Content in Dried Capsule (%)	Immobilized Amount (mg/g$_{capsules}$)	Concentration on Capsule (mg/dm^2)
C1	0	0.57 ± 0.16	0.79 ± 0.24
C2	2.4	0.80 ± 0.18	1.13 ± 0.23
C3	4.8	0.88 ± 0.09	1.26 ± 0.12
C4	9.1	1.03 ± 0.17	1.56 ± 0.13
C5	20	1.36 ± 0.19	1.83 ± 0.21

Figure 6, as an example, provides ESEM micrographs of surface and cross-section morphologies of the C5 capsule before and after enzyme immobilization. From the images, it can be observed that the internal morphology after enzyme immobilization seems to be more compacted while the external capsules surface became dense. These results suggest that the enzyme penetrated the capsule wall (membrane) morphology [48], and they are filled in the porous structure [49], closing the surface pores [50], making the capsule surface dense and homogeneous.
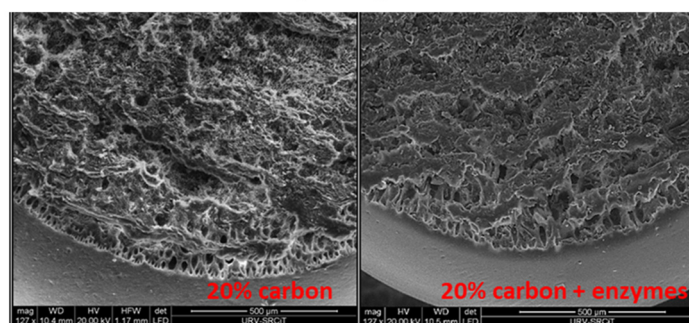

Figure 6. ESEM micrographs of surface and cross-section morphologies of C5 capsule before and after enzyme immobilization.

Finally, activity of immobilized enzymes on the C5 capsules was determined by cellulose hydrolysis to glucose (Scheme 1) following the Reducing Sugar DNS method. As it is illustrated in the Scheme 1, enzymatic hydrolysis involves the cleavage of β-1,4-glycosidic bonds of cellulose and generates glucose [51]. Our results demonstrated that 10 g of C5 enzyme immobilized capsules were able to hydrolyze 1 g/L of carboxymethyl cellulose sodium salt (during a 24 h reaction carried out at 50 °C), producing 107 mg/L of glucose. In order to check if the recycled capsules maintain their activity, the capsules were reused in three additional, independent hydrolase tests, producing 78, 76, and 79 mg/L of glucose in each reaction batch. Generally, cellulolytic enzymes tend to have optimal activity in the acidic to neutral pH range. For example, free cellulase enzymes typically show optimal activity around pH 4.4 to 5.01, while immobilized cellulase enzymes exhibit

optimal activity around pH 5.0. Thus, following the literature [12,52], we selected this pH 5 value to carry out the cellulose hydrolysis experiments.
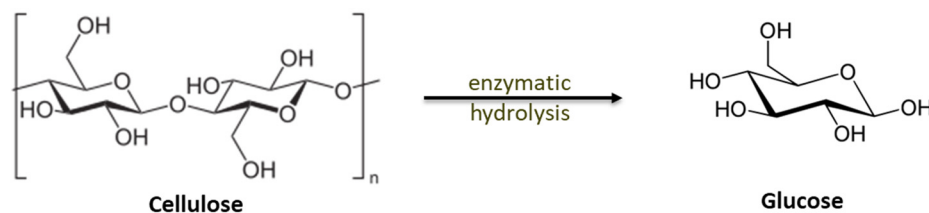
Scheme 1. A scheme of cellulose hydrolysis by enzyme.

Figure 7 shows that the activity of non-immobilized enzyme is approximately five times higher than the immobilized one on C5 capsules. A quantum and molecular mechanics study, performed by Petrosino et al. [53] on enzyme adsorption on polysulfone surface, suggests that the binding site of the immobilized enzyme can be less accessible, with respect to the pristine enzyme, due to the steric hindrance of the polymer surface; thus, a reduction in the enzyme efficiency can be expected. On the other hand, it is important to highlight that the immobilized enzyme can be recovered from the reactor by separation methods and it can be reused. Considering that current processes employed in the paper industry do not involve pure enzyme recovery from the production (they are considered bio-waste), the easy and cheap separation method of capsules with immobilized enzymes could have a significant impact on the decrease in paper production cost as well as on environmental aspect of bio-waste reduction. Moreover, the results presented in Figure 6 suggest that the immobilized enzyme are stable, and they were not significantly washed out from the capsule structure during their application in cellulose hydrolysis.
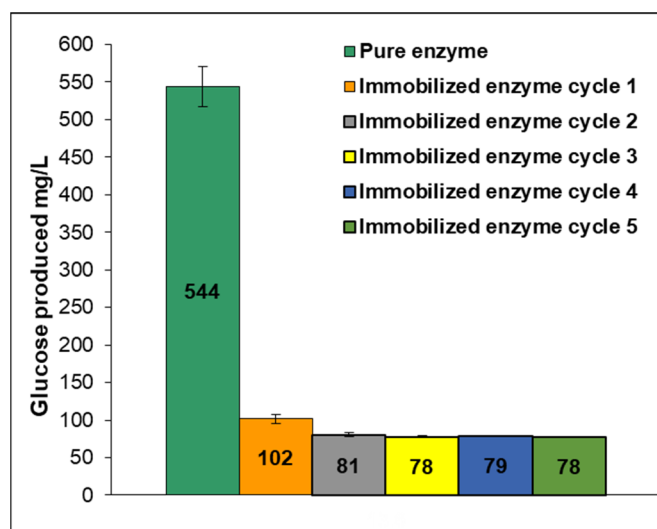

Figure 7. Results of cellulose hydrolysis by pure and immobilized enzymes.

4. Conclusions

Five types of polysulfone-based capsules were successfully prepared by phase inversion precipitation method. Four of them (C2–C5) contain activated carbon nanoparticles into their matrix, in a concentration range between 2.4 and 20 wt%. Capsules morphologies change with the increase in activated carbon content growth, leading to porous diameter decrease. Higer content of activated carbon in polymeric capsule matrix significantly influences on physical immobilization of enzyme. Hydrolysis of carboxymethyl cellulose to glucose in the presence of immobilized enzymes in the polysulfone-activated carbon capsule, monitored Reducing Sugar DNS test, confirmed the immobilized enzyme activity.

5. Patents

ENZYMATIC BEAD WIPO Patent Application WO/2022/053466.

Conflicts of Interest: The authors declare no conflicts of interest.

References

1. Mao, S.; Jiang, J.; Xiong, K.; Chen, Y.; Yao, Y.; Liu, L.; Liu, H.; Li, X. Enzyme Engineering: Performance Optimization, Novel Sources, and Applications in the Food Industry. *Foods* **2024**, *13*, 3846. [CrossRef]
2. Belorkar, S.A.; Jogaiah, S. Chapter 1—Enzymes—Past, Present, and Future. In *Protocols and Applications in Enzymology*; Belorkar, S.A., Jogaiah, S., Eds.; Academic Press: Cambridge, MA, USA, 2022; pp. 1–15, ISBN 978-0-323-91268-6.
3. Tamanoi, F. Chapter One—History of The Enzymes: 1950–2023. In *The Enzymes*; Kaguni, L.S., Tamanoi, F., Eds.; History of Current Topics and Future Perspectives; Academic Press: Cambridge, MA, USA, 2023; Volume 54, pp. 3–11.
4. Mannaa, M.; Han, G.; Seo, Y.-S.; Park, I. Evolution of Food Fermentation Processes and the Use of Multi-Omics in Deciphering the Roles of the Microbiota. *Foods* **2021**, *10*, 2861. [CrossRef] [PubMed]
5. Costa, I.O.; Morais, J.R.F.; de Medeiros Dantas, J.M.; Gonçalves, L.R.B.; dos Santos, E.S.; Rios, N.S. Enzyme Immobilization Technology as a Tool to Innovate in the Production of Biofuels: A Special Review of the Cross-Linked Enzyme Aggregates (CLEAs) Strategy. *Enzym. Microb. Technol.* **2023**, *170*, 110300. [CrossRef] [PubMed]
6. Maske, B.L.; de Melo Pereira, G.V.; Vale, A.d.S.; de Carvalho Neto, D.P.; Karp, S.G.; Viesser, J.A.; De Dea Lindner, J.; Pagnoncelli, M.G.; Soccol, V.T.; Soccol, C.R. A Review on Enzyme-Producing Lactobacilli Associated with the Human Digestive Process: From Metabolism to Application. *Enzym. Microb. Technol.* **2021**, *149*, 109836. [CrossRef]
7. Garg, K.; Sehgal, R.; Sharma, D.; Gupta, R. Polyhydroxyalkanoates as Matrices for Enzyme Immobilization: In Vivo and In Vitro Approaches. *Process Biochem.* **2024**, *147*, 530–542. [CrossRef]
8. Almulaiky, Y.Q.; Alkabli, J.; El-Shishtawy, R.M. Improving Enzyme Immobilization: A New Carrier-Based Magnetic Polymer for Enhanced Covalent Binding of Laccase Enzyme. *Int. J. Biol. Macromol.* **2024**, *282*, 137362. [CrossRef]
9. Guisan, J.M.; Fernandez-Lorente, G.; Rocha-Martin, J.; Moreno-Gamero, D. Enzyme Immobilization Strategies for the Design of Robust and Efficient Biocatalysts. *Curr. Opin. Green Sustain. Chem.* **2022**, *35*, 100593. [CrossRef]
10. Křen, V.; Bojarová, P. Biocatalysis: "A Jack of All Trades...". *Int. J. Mol. Sci.* **2020**, *21*, 5115. [CrossRef]
11. Sheldon, R.A.; Basso, A.; Brady, D. New Frontiers in Enzyme Immobilisation: Robust Biocatalysts for a Circular Bio-Based Economy. *Chem. Soc. Rev.* **2021**, *50*, 5850–5862. [CrossRef]
12. Berlowska, J.; Cieciura-Włoch, W.; Kalinowska, H.; Kregiel, D.; Borowski, S.; Pawlikowska, E.; Binczarski, M.; Witonska, I. Enzymatic Conversion of Sugar Beet Pulp: A Comparison of Simultaneous Saccharification and Fermentation and Separate Hydrolysis and Fermentation for Lactic Acid Production. *Food Technol. Biotechnol.* **2018**, *56*, 188–196. [CrossRef]
13. Maghraby, Y.R.; El-Shabasy, R.M.; Ibrahim, A.H.; Azzazy, H.M.E.-S. Enzyme Immobilization Technologies and Industrial Applications. *ACS Omega* **2023**, *8*, 5184–5196. [CrossRef] [PubMed]
14. Olkiewicz, M.; Tylkowski, B.; Montornés, J.M.; Garcia-Valls, R.; Gulaczyk, I. Modelling of Enzyme Kinetics: Cellulose Enzymatic Hydrolysis Case. *Phys. Sci. Rev.* **2022**, *7*, 901–921. [CrossRef]
15. Nguyen, H.H.; Lee, S.H.; Lee, U.J.; Fermin, C.D.; Kim, M. Immobilized Enzymes in Biosensor Applications. *Materials* **2019**, *12*, 121. [CrossRef] [PubMed]
16. Rodrigues, J.G.C.; Cardoso, F.V.; Duvoisin Junior, S.; Machado, N.T.; Albuquerque, P.M. Endomelanconiopsis Endophytica Lipase Immobilized in Calcium Alginate for Production of Biodiesel from Waste Cooking Oil. *Energies* **2024**, *17*, 5520. [CrossRef]
17. Basso, A.; Serban, S. Industrial Applications of Immobilized Enzymes—A Review. *Mol. Catal.* **2019**, *479*, 110607. [CrossRef]

18. Santos, M.P.F.; de Souza Junior, E.C.; Villadóniga, C.; Vallés, D.; Castro-Sowinski, S.; Bonomo, R.C.F.; Veloso, C.M. Proteases: Importance, Immobilization Protocols, Potential of Activated Carbon as Support, and the Importance of Modifying Supports for Immobilization. *BioTech* **2024**, *13*, 13. [CrossRef] [PubMed]

19. Antanasković, A.; Lopičić, Z.; Dimitrijević-Branković, S.; Ilić, N.; Adamović, V.; Šoštarić, T.; Milivojević, M. Biochar as an Enzyme Immobilization Support and Its Application for Dye Degradation. *Processes* **2024**, *12*, 2418. [CrossRef]

20. de Almeida, L.C.; Andrade, E.L.O.; Santos, J.C.B.; Santos, R.M.; Fricks, A.T.; Freitas, L.d.S.; Lima, Á.S.; Pereira, M.M.; Soares, C.M.F. Novel Nanobiocatalyst Constituted by Lipase from Burkholderia Cepacia Immobilized on Graphene Oxide Derived from Grape Seed Biochar. *C* **2023**, *9*, 12. [CrossRef]

21. Bialas, F.; Reichinger, D.; Becker, C.F.W. Biomimetic and Biopolymer-Based Enzyme Encapsulation. *Enzyme Microb. Technol.* **2021**, *150*, 109864. [CrossRef] [PubMed]

22. Enzyme-Polymer Conjugates for Tuning, Enhancing, and Expanding Biocatalytic Activity—Heredero—2023—ChemBioChem—Wiley Online Library. Available online: https://chemistry-europe-onlinelibrary-wiley-com.sabidi.urv.cat/doi/10.1002/cbic.2022 00611 (accessed on 13 November 2024).

23. Yuan, Y.; Shen, J.; Salmon, S. Developing Enzyme Immobilization with Fibrous Membranes: Longevity and Characterization Considerations. *Membranes* **2023**, *13*, 532. [CrossRef] [PubMed]

24. Rodriguez-Abetxuko, A.; Sánchez-deAlcázar, D.; Muñumer, P.; Beloqui, A. Tunable Polymeric Scaffolds for Enzyme Immobilization. *Front. Bioeng. Biotechnol.* **2020**, *8*, 830. [CrossRef] [PubMed]

25. Dong, X.; Al-Jumaily, A.; Escobar, I.C. Investigation of the Use of a Bio-Derived Solvent for Non-Solvent-Induced Phase Separation (NIPS) Fabrication of Polysulfone Membranes. *Membranes* **2018**, *8*, 23. [CrossRef] [PubMed]

26. Tylkowski, B.; Carosio, F.; Castañeda, J.; Alongi, J.; García-Valls, R.; Malucelli, G.; Giamberini, M. Permeation Behavior of Polysulfone Membranes Modified by Fully Organic Layer-by-Layer Assemblies. *Ind. Eng. Chem. Res.* **2013**, *52*, 16406–16413. [CrossRef]

27. Sauers, M.E.; McKenna, L.A.; Merriam, C.N. Polysulfone—Early Market Development Activities. In Proceedings of the High Performance Polymers: Their Origin and Development, New York, NY, USA, 15–18 April 1986; Seymour, R.B., Kirshenbaum, G.S., Eds.; Springer: Dordrecht, The Netherlands, 1986; pp. 159–168.

28. Khoury, J.M.; Hamam, R.N.; Chan, T.K.; Ghanem, R.C.; de la Cruz, J.; Azar, D.T. 27—Intracorneal Alloplastic Inclusions and Femtosecond Laser Lamellar Surgery. In *Refractive Surgery*, 2nd ed.; Azar, D.T., Ed.; Mosby: Edinburgh, Scotland, 2007; pp. 363–372, ISBN 978-0-323-03599-6.

29. Machado, D.B.; Skoronski, E.; Soares, C.; Padoin, N. Immobilisation of Phosphonium-Based Ionic Liquid in Polysulfone Capsules for the Removal of Phenolic Compounds, with an Emphasis on 2,4-Dichlorophenol, in Aqueous Solution. *J. Environ. Manag.* **2021**, *291*, 112670. [CrossRef]

30. Kazak, O.; Tor, A.; Akin, I.; Arslan, G. Preparation of New Polysulfone Capsules Containing Cyanex 272 and Their Properties for Co(II) Removal from Aqueous Solution. *J. Environ. Chem. Eng.* **2015**, *3*, 1654–1661. [CrossRef]

31. Panisello, C.; Peña, B.; Gumí, T.; Garcia-Valls, R. Polysulfone Microcapsules with Different Wall Morphology. *J. Appl. Polym. Sci.* **2013**, *129*, 1625–1636. [CrossRef]

32. Haponska, M.; Trojanowska, A.; Nogalska, A.; Jastrzab, R.; Gumi, T.; Tylkowski, B. PVDF Membrane Morphology—Influence of Polymer Molecular Weight and Preparation Temperature. *Polymers* **2017**, *9*, 718. [CrossRef] [PubMed]

33. Duraikkannu, S.L.; Castro-Muñoz, R.; Figoli, A. A Review on Phase-Inversion Technique-Based Polymer Microsphere Fabrication. *Colloid Interface Sci. Commun.* **2021**, *40*, 100329. [CrossRef]

34. Purkait, M.K.; Sinha, M.K.; Mondal, P.; Singh, R. (Eds.) Chapter 1—Introduction to Membranes. In *Interface Science and Technology*; Stimuli Responsive Polymeric Membranes; Elsevier: Amsterdam, The Netherlands, 2018; Volume 25, pp. 1–37.

35. Bogdanowicz, K.A.; Tylkowski, B.; Giamberini, M. Preparation and Characterization of Light-Sensitive Microcapsules Based on a Liquid Crystalline Polyester. *Langmuir* **2013**, *29*, 1601–1608. [CrossRef]

36. Tylkowski, B.; Trojanowska, A.; Giamberini, M.; Tsibranska, I.; Nowak, M.; Marciniak, Ł.; Jastrzab, R. Microencapsulation in Food Chemistry. *J. Membr. Sci. Res.* **2017**, *3*, 265–271. [CrossRef]

37. Nogalska, A. Ambient Carbon Dioxide Capture and Conversion via Membranes. Ph.D. Thesis, Universitat Rovira i Virgili, Reus, Spain, 2018.

38. Miller, G.L. Use of Dinitrosalicylic Acid Reagent for Determination of Reducing Sugar. *Anal. Chem.* **1959**, *31*, 426–428. [CrossRef]

39. Sharma, M.; Alves, P.; Gando-Ferreira, L.M. Effect of Activated Carbon Nanoparticles on the Performance of PES Nanofiltration Membranes to Separate Kraft Lignin from Black Liquor. *J. Water Process Eng.* **2023**, *52*, 103487. [CrossRef]

40. Hosseini, S.M.; Amini, S.H.; Khodabakhshi, A.R.; Bagheripour, E.; Van der Bruggen, B. Activated Carbon Nanoparticles Entrapped Mixed Matrix Polyethersulfone Based Nanofiltration Membrane for Sulfate and Copper Removal from Water. *J. Taiwan Inst. Chem. Eng.* **2018**, *82*, 169–178. [CrossRef]

41. Tan, X.; Rodrigue, D. A Review on Porous Polymeric Membrane Preparation. Part I: Production Techniques with Polysulfone and Poly (Vinylidene Fluoride). *Polymers* **2019**, *11*, 1160. [CrossRef]

42. Torras, C.; Ferrando, F.; Paltakari, J.; Garcia-Valls, R. Performance, Morphology and Tensile Characterization of Activated Carbon Composite Membranes for the Synthesis of Enzyme Membrane Reactors. *J. Membr. Sci.* **2006**, *282*, 149–161. [CrossRef]

43. Torras, C.; Torné, V.; Fierro, V.; Montané, D.; Garcia-Valls, R. Polymeric Composite Membranes Based on Carbon/PSf. *J. Membr. Sci.* **2006**, *273*, 38–46. [CrossRef]

44. Anadão, P.; Sato, L.F.; Wiebeck, H.; Valenzuela-Díaz, F.R. Polysulfone Activated Carbon Composite Membranes. In *Materials Science Forum*; ResearchGate; Trans Tech Publications Ltd.: Stäfa, Switzerland, 2024. [CrossRef]

45. Nayak, R.J.; Khare, P.K.; Nayak, J.G. Analysis of Pure and Malachite Green Doped Polysulfone Sample Using FT-IR Technique. *AIP Conf. Proc.* **2018**, *1953*, 100057. [CrossRef]

46. Figueiredo, J.L.; Pereira, M.F.R.; Freitas, M.M.A.; Órfão, J.J.M. Modification of the Surface Chemistry of Activated Carbons. *Carbon* **1999**, *37*, 1379–1389. [CrossRef]

47. Faiz Haddad, H.; Prabhu, A.; Al Shoaibi, A.; Srinivasakannan, C. Assessment of Various Carbon-Based Adsorbents for Separation of BTX from Aqueous Solution. *Water Supply* **2015**, *15*, 649–655. [CrossRef]

48. Chen, P.-C.; Zhu, X.-Y.; Li, J.; Huang, X.-J. Enzyme Immobilization on Membrane and Its Application in Bioreactors. In *Biocatalysis and Nanotechnology*; Jenny Stanford Publishing: Singapore, 2017; ISBN 978-1-315-19660-2.

49. Dalvie, S.K.; Baltus, R.E. Distribution of Immobilized Enzymes on Porous Membranes. *Biotechnol. Bioeng.* **1992**, *40*, 1173–1180. [CrossRef] [PubMed]

50. McShane, M.J. Enzyme Immobilization in Polyelectrolyte Microcapsules. In *Enzyme Stabilization and Immobilization: Methods and Protocols*; Minteer, S.D., Ed.; Humana Press: Totowa, NJ, USA, 2011; pp. 147–154, ISBN 978-1-60761-895-9.

51. Amândio, M.S.T.; Rocha, J.M.S.; Xavier, A.M.R.B. Enzymatic Hydrolysis Strategies for Cellulosic Sugars Production to Obtain Bioethanol from Eucalyptus Globulus Bark. *Fermentation* **2023**, *9*, 241. [CrossRef]

52. Samaratunga, A.; Kudina, O.; Nahar, N.; Zakharchenko, A.; Minko, S.; Voronov, A.; Pryor, S.W. Modeling the Effect of pH and Temperature for Cellulases Immobilized on Enzymogel Nanoparticles. *Appl. Biochem. Biotechnol.* **2015**, *176*, 1114–1130. [CrossRef] [PubMed]

53. Petrosino, F.; Curcio, S.; Chakraborty, S.; De Luca, G. Enzyme Immobilization on Polymer Membranes: A Quantum and Molecular Mechanics Study. *Computation* **2019**, *7*, 56. [CrossRef]